International Journal of Thermophysics, Vol. 12, No. 6, 1991

Photoacoustic Determination of Thermophysical Properties of Thin Metallic Plates Using Parameter Estimation

S. W. Kim,[1,2] J. Lee,[1] and R. E. Taylor[1]

Received February 28, 1991

The phase and the amplitude of the photoacoustic signal were measured as a function of chopping frequency for several kinds of widely used thin metallic plates (stainless steel 304, brass, aluminum, and copper) attached to plexiglass backing. The experimental data have been analyzed systematically by parameter estimation technique based on the two-layer model developed from Rosencwaig–Gersho (R-G) theory. Using this analysis, the values of thermal diffusivity and thermal effusivity of the materials have been determined.

KEY WORDS: parameter estimation; photoacoustic technique; thermal diffusivity; thermal effusivity.

1. INTRODUCTION

Gas photoacoustic (PA) techniques have been applied to a number of fields since the general PA theory was established, especially in the area of the measurement of thermophysical properties of thin films [1–3].

The understanding of heat transfer through thin plates or films applied to a substrate has become increasingly important in technological applications. Early applications of the PA effect to the measurement of thermal diffusivity of thin films were made by Adams and Kirkbright [4]. Mandelis et al. [5] and Tominaga and Ito [6] extended the R-G theory to a two-layer sample system. Also, Lachaine and Poulet [7] measured the thermal properties of a thin polymer film and Benedeto and Spagnolo [8] measured the thermal effusivity of thin plates.

[1] Thermophysical Properties Research Laboratory, School of Mechanical Engineering, Purdue University, West Lafayette, Indiana 47906, U.S.A.

[2] On leave from Temperature Laboratory, Korea Standards Research Institute, P.O. Box 3, Taedok Science Town, Taejon 305-606, Korea.

0195-928X/91/1100-1063$06.50/0

There are two kinds of modes in PA measurement, namely, front surface excitation (FSE) and rear surface excitation (RSE). Using the FSE mode, Swimm [9] showed that the measurements can be applied to 2-μm-thick As_2Se_3 thin film deposited on a thick KCl substrate at chopping frequencies up to 5 kHz. The RSE mode has been applied to the measurement of the thermal diffusivity of polymer film ($\sim 10\,\mu$m) on copper substrates at chopping frequencies up to 200 Hz [4]. One limitation of the RSE mode is that a strong heat source such as a laser beam is required to get detectable signals [10]. Both the phase and the amplitude of the PA signal in each mode can provide information on thermophysical properties.

In this work, we measured both the phase and the amplitude of the photoacoustic signal by the FSE mode for thin metal plates attached to plexiglass backing. We analyzed the experiments systematically by using a parameter estimation technique [11] and obtained the values of thermal diffusivity and thermal effusivity of the samples.

2. EXPRESSIONS FOR PHASE AND AMPLITUDE OF PA SIGNAL

For the FSE mode of an opaque film on a backing material, the expressions for the phase variation [Eq. (1)] and amplitude variation of the PA signal [Eq. (2)] can be derived from R-G theory [9, 10].

$$\Phi_{\mathrm{fs}} = \tan^{-1}(m \tan Y) - \tan^{-1}(m^{-1} \tan Y) \tag{1}$$

$$A_{\mathrm{fs}} = \frac{A_0}{2Y^2}\left[\frac{\{(1+g)\,e^{Y}+(1-g)\,e^{-Y}\}^2\cos^2 Y + \{(1+g)\,e^{Y}-(1-g)\,e^{-Y}\}^2\sin^2 Y}{\{(1+g)\,e^{Y}-(1-g)\,e^{-Y}\}^2\cos^2 Y + \{(1+g)\,e^{Y}+(1-g)\,e^{-Y}\}^2\sin^2 Y}\right]^{1/2} \tag{2}$$

where

$$m = \frac{(1+g)\,e^{Y}+(1-g)\,e^{-Y}}{(1+g)\,e^{Y}-(1-g)\,e^{-Y}} \tag{3}$$

$$g = \varepsilon_{\mathrm{b}}/\varepsilon_{\mathrm{s}} \qquad (\mathrm{b} = \text{backing material, s} = \text{sample}) \tag{4}$$

$$\varepsilon_i = k_i/\sqrt{\alpha_i} \qquad (k_{\mathrm{i}} = \text{thermal conductivity}, \alpha_{\mathrm{i}} = \text{thermal diffusivity}) \tag{5}$$

$$f_{\mathrm{c}} = \alpha_{\mathrm{s}}/t_{\mathrm{s}}^2 \qquad (t_{\mathrm{s}} = \text{thickness of sample}) \tag{6}$$

$$Y = \sqrt{\pi f/f_{\mathrm{c}}} \qquad (f = \text{chopping frequency}) \tag{7}$$

where A_0 is the amplitude constant which is independent of chopping frequency, ε_i is the thermal effusivity, f_c is the characteristic frequency of the sample, and g is the effusivity ratio of backing to sample.

Figures 1 and 2 show the variations of phase and amplitude with different g values, as a function of $(f/f_c)^{1/2}$, respectively. For a variation of g, the change of phase is much greater than that of the amplitude. This means that the phase is more sensitive to g than the amplitude.

3. PARAMETER ESTIMATION

Parameter estimation is a powerful technique that can use all the available data points and provides statistical means to analyze the experiment [12]. Parameter estimation (PE) [11] procedure was the method of choice to get optimum values for the f_c and g values governed by Eq. (1) and f_c, g, and A_0 values governed by Eq. (2). A nonlinear PE algorithm NL2SOL, developed by Dennis et al. [13, 14], was used in this work.

The reliability of the estimated parameters obtained by using NL2SOL software depends on the sensitivity coefficient (SC) of each parameter. The

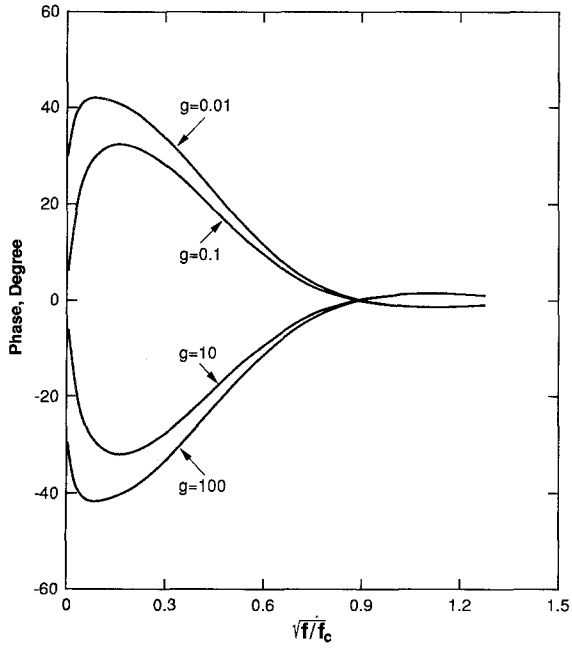

Fig. 1. Phase shifts of a photoacoustic signal as a function of $(f/f_c)^{1/2}$ with different g values.

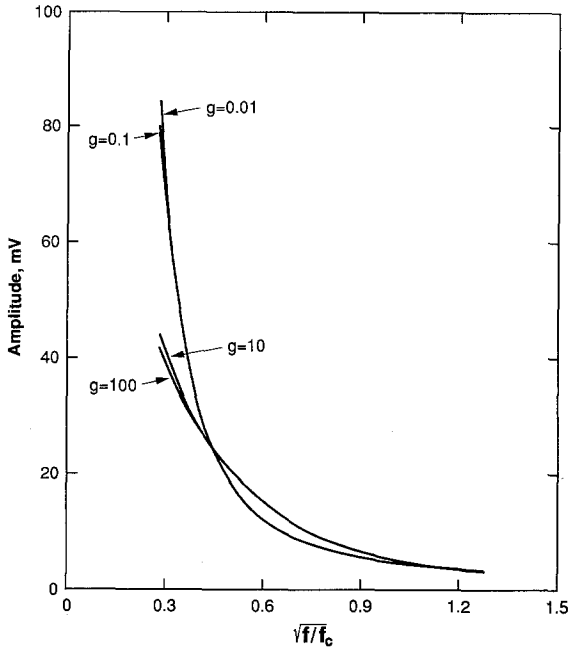

Fig. 2. Amplitude variations of a photoacoustic signal as a function of $(f/f_c)^{1/2}$ with different g values.

first derivative for the expressions of phase or amplitude of the signal with respect to the parameter is the SC, and when normalized to units of the phase (degree) or amplitude (mV), they appear as

$$\Gamma_j = \beta_j \frac{\partial S}{\partial \beta_j} \tag{8}$$

where Γ_j is the normalized sensitivity coefficient, S is either the phase or the amplitude of the signal, β_j is the parameter, and j is the index of parameters [12]. The SCs for the parameters can provide a considerable amount of insight as to the adequacy of the model. If the model behaves similarly with a change in one parameter as it does with a change in another parameter, then the parameters are correlated, or dependent to some degree.

Figure 3 presents the SCs for the case of phase measurement at $f_c = 177.75$ Hz and $g = 0.014$. The SC for f_c rapidly increases from low frequency to about half of the f_c value and then smoothly decreases. The SC for g is always close to zero (independent of the frequency). These mean that f_c and g are not strongly dependent and reliable values of both

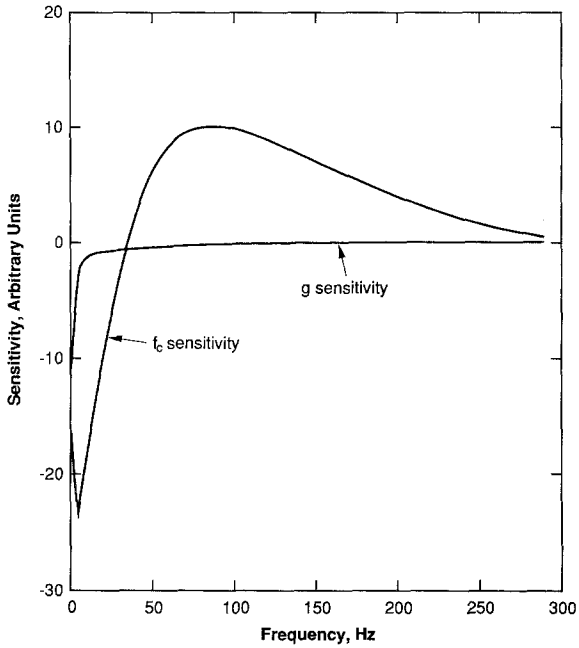

Fig. 3. Sensitivity coefficients for the phase measurement ($f_c = 177.75$ Hz, $g = 0.014$).

parameters can be estimated. Figure 4 shows the variation of SCs for the amplitude measurement at $f_c = 177.75$ Hz, $A_0 = 30$, and $g = 0.014$. The SC for g is always near-zero. However, the SCs for f_c and A_0 show nearly the same features. This indicates that f_c and A_0 are strongly dependent and it is hard to get reliable estimations for both f_c and A_0 simultaneously from the analysis. However, if f_c or A_0 can be obtained independently, then remaining two parameters are not strongly dependent and reliable values of both parameters can be estimated.

The correlation coefficient (CC) is a quantitative measure of how β_j and β_k are related (β_j and β_k are the jth and kth parameters) [11]. The CC physically has the range of $(-1 \leqslant \rho_{jk} \leqslant 1)$, where ρ_{jk} is the CC of β_j and β_k. The significance of ρ_{jk} is that it describes the degree of linear dependency of the two parameters. Completely linear dependency is implied when ρ_{jk} approaches ± 1. The CC is calculated from the variance–covariance matrix by the following relation [11]:

$$\rho_{jk} = \frac{\operatorname{cov}(\hat{\beta}_j, \hat{\beta}_k)}{\operatorname{var}(\hat{\beta}_j)\operatorname{var}(\hat{\beta}_k)} \tag{9}$$

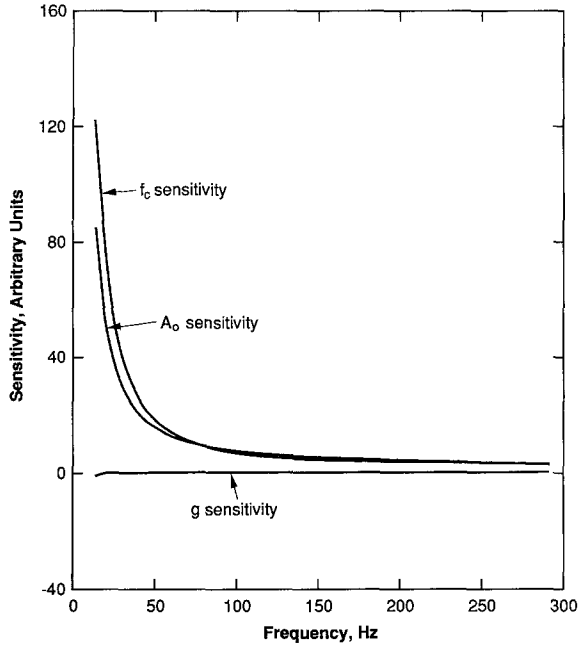

Fig. 4. Sensitivity coefficients for the amplitude measurement ($f_c = 177.75$ Hz, $A_0 = 30$, and $g = 0.014$).

where $\hat{\beta}_j$ and $\hat{\beta}_k$ are the jth and kth optimal parameters, respectively, $\text{cov}(\hat{\beta}_j, \hat{\beta}_k)$ is the covariance of the two optimal parameters, and $\text{var}(\hat{\beta}_j)$ is the variance of the optimal parameter. The calculated CC value of f_c and g for the case of Fig. 3 is -0.577. This means that the two parameters do not have a strong correlation. In Fig. 4, the CC value of f_c and A_0 is -0.992, that of f_c and g is 0.853, and that of A_0 and g is -0.781. These mean that A_0 and g have a moderate correlation, but the other two correlations are relatively strong.

Table I shows the calculated values of CC in both the phase and the amplitude measurements for different values of f_c and g. In phase measurement, for the same values of g, the absolute values of CC for $f_c = 500$ Hz are smaller than those for $f_c = 50$ and 200 Hz. For the same f_c value, when $g > 1.0$, the absolute values of CC are smaller than the case of $g < 1.0$. These mean that the model for the phase measurement is more reliable when f_c is several hundred hertz and when the condition of $\varepsilon_s < \varepsilon_b$ is satisfied.

For the case of amplitude measurement, the values of CC were calculated when A_0 was 30.0 (the value of CC is independent of the value

Table I. Calculated Values of the Correlation Coefficient in the Phase and Amplitude Measurement for Different Values of f_c and g

f_c (Hz)	g	Phase measurement	Amplitude measurement		
		$f_c g$	$f_c A_0$	$f_c g$	$A_0 g$
50	0.01	−0.582	−0.994	0.884	−0.829
	0.10	−0.358	−0.995	0.882	−0.833
	10.00	0.064	−0.982	−0.701	0.793
	100.00	0.073	−0.977	−0.752	0.839
200	0.01	−0.352	−0.995	0.855	−0.810
	0.10	−0.348	−0.997	−0.639	0.693
	10.00	0.064	−0.971	−0.302	0.501
	100.00	0.111	−0.963	−0.631	0.786
500	0.01	−0.289	−0.991	0.843	−0.763
	0.10	−0.342	−0.993	0.827	−0.754
	10.00	0.062	−0.986	−0.842	0.910
	100.00	0.116	−0.980	−0.853	0.925

of A_0). The trend is similar to phase measurement, but when f_c is 500 Hz the absolute values of CC become large for $g > 0.1$. Table I also shows that the CC values of f_c and A_0 are always near -1.0. This means that the correlation between the two parameters is very strong. In this case if we can independently obtain either f_c or A_0, more reliable values can be obtained for the remaining parameters as predicted in Fig. 4.

4. EXPERIMENTS

The experimental setup is shown in Fig. 5. The heating beam from a mercury arc lamp (200 W) is absorbed by the sample placed in the PA cell. The beam is modulated by a mechanical chopper (SRS 540) whose chopping frequency can be varied from a few hertz to a few kilohertz and controlled by a personal computer. The beam size on the sample surface is fixed to be a half-inch by a condensing lens and iris. For the detection and amplification of the PA signal, we have used the half-inch microphone (ACO 7047), whose sensitivity is 40 mV/Pa, and preamplifier (KEITHLEY 103A), respectively. A dual-phase lock-in amplifier (SR530) is used to analyze the phase and amplitude of the signal.

Figure 5 also shows the design of the PA cell. To minimize the stray light effect and other background noises, the cell was made of plexiglass, whose absorption is negligible [15]. In the cell there are two chambers,

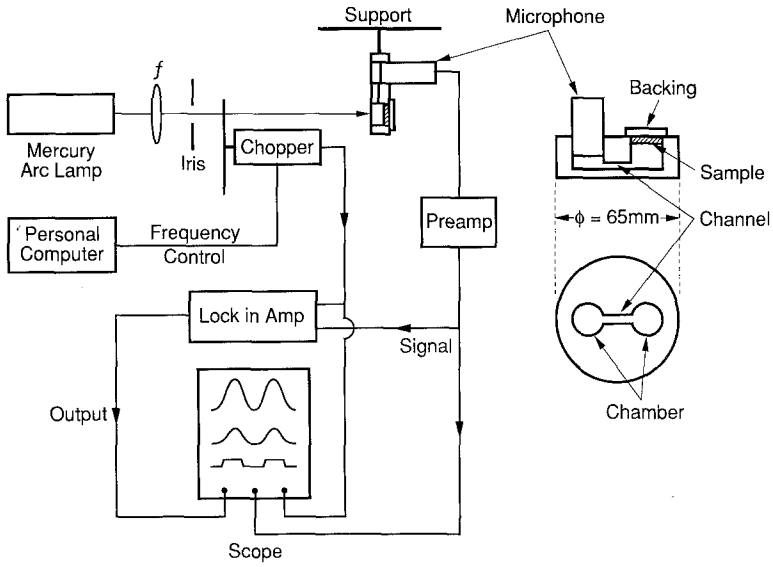

Fig. 5. Schematic diagram of the experimental setup and the design of a photoacoustic cell.

one is for the sample and the other is for the microphone. The two chambers are connected by a narrow channel. The calculated Helmholtz resonance frequency [16] for this cell was 642 Hz. Therefore, the effect of the resonance frequency to the signal can be neglected because the interesting frequency region is from a few hertz to about 300 Hz.

The samples we used were (1) stainless steel 304 ($l_s = 0.386$ mm), (2) stainless steel 304 ($l_s = 0.274$ mm), (3) brass ($l_s = 0.528$ mm), (4) aluminum ($l_s = 1.580$ mm), and (5) copper ($l_s = 0.795$ mm). The diameters of all the samples were 12.5 mm. To enhance the signal-to-noise ratio, the front surfaces of the samples were coated with graphite (thickness, < 0.1 μm). Also, in order to avoid the drum effect [10], the samples were attached to the plexiglass backing with vacuum grease (Dow Corning High Vacuum Grease).

The phase and amplitude of PA signal were measured simultaneously by changing the chopping frequency from several hertz to about 1.3 times the f_c value [f_c value was roughly estimated by Eq. (6) with the thickness of the sample and literature value of α_s [17, 18]]. In order to eliminate parasitic phase variations in phase measurement, additional calibration experiment was made [9]. We measured the phase variation of a thermally thick calibration sample (graphite $l_s = 5$ mm) and subtracted this variation from the measured phase value of the sample to get the corrected phase variation.

5. RESULTS AND DISCUSSION

Since the thickness of the vacuum grease layer between the sample layer and the backing material is very thin, we assumed that the effect of the vacuum grease layer can be ignored [4, 19] and the two-layer model is applicable. In order to investigate the effect of backing, we measured the phase variation of Sample (2) for two backing materials (plexiglass and aluminum). The results are shown in Fig. 6 with the theoretical curves calculated from the two-layer model. Figure 6 shows that the signal of PA is strongly affected by the backing material. The estimated values of thermal diffusivity for Sample (2) is 0.041 and 0.042 $cm^2 \cdot s^{-1}$ using plexiglass and aluminum backings, respectively. These values agree well with the literature values [17, 18].

The experiments were performed five times for each sample. Figure 7 shows the results of phase measurement (data points and theoretical curves) for Sample (3) and Sample (5). The theoretical curves were obtained by using the two-parameter (f_c and g) estimation procedure. Table II shows the comparison of the estimated values of thermal diffusivity and thermal effusivity with the literature values [18, 19]. In the calculation of

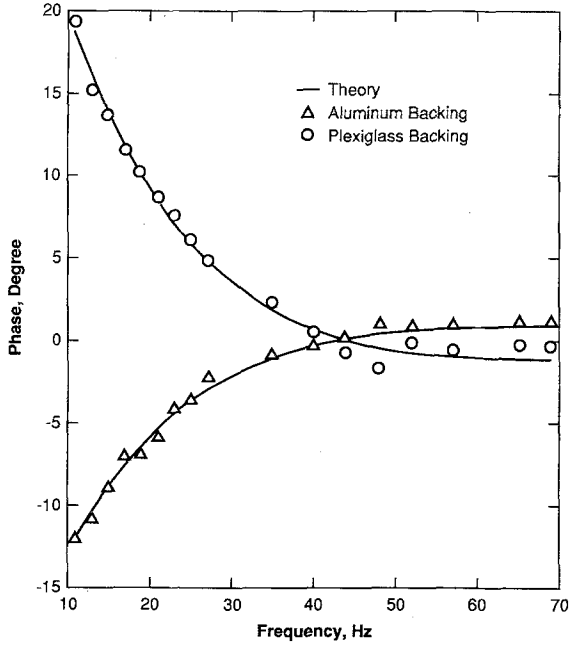

Fig. 6. Phase variations of a photoacoustic signal with different backing materials. Sample is stainless steel 304 ($l_s = 0.274$ mm).

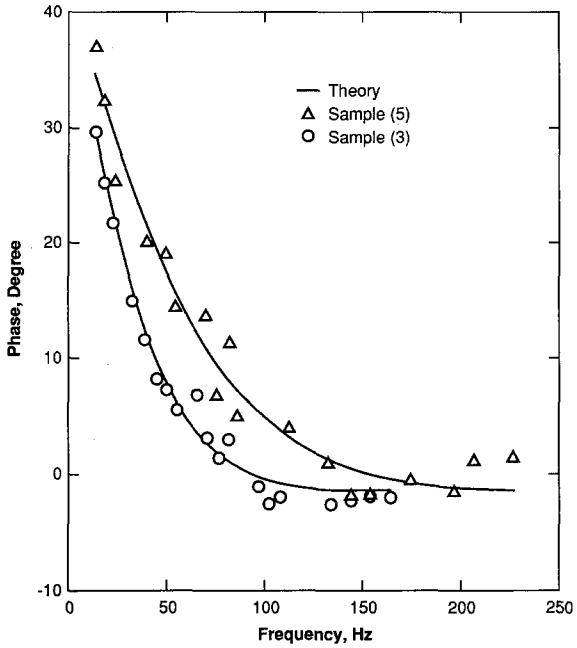

Fig. 7. Experimental data with the theoretical curve fit using the parameter estimation of f_c and g in phase measurement. Sample (3): $f_c = 112.27$ Hz, $g = 0.030$. Sample (5): $f_c = 183.54$ Hz, $g = 0.016$.

Table II. Thermal Diffusivity and Thermal Effusivity Values Obtained from the Phase Measurement Compared with the Values Quoted in the Literature

Sample No.	$\alpha_s(cm^2 \cdot s^{-1})$		$\varepsilon_s(W \cdot s^{1/2} \cdot cm^{-2} \cdot K^{-1})$	
	Measured	Literature[a]	Measured	Literature[b]
1	0.043 ± 0.003	0.039	0.55 ± 0.06	0.689
2	0.041 ± 0.039	0.039	0.49 ± 0.05	0.689
3	0.313 ± 0.008	0.340	1.6 ± 0.3	1.930
4	0.94 ± 0.02	0.970	2.1 ± 0.3	2.193
5	1.16 ± 0.03	1.20	3.0 ± 0.4	3.466

[a] Quoted from Refs. 17 and 18.
[b] Computed from values of thermal conductivity and thermal diffusivity [17, 18].

Table III. Thermal Diffusivity and Thermal Effusivity Values Obtained from the Amplitude Measurement by Three-Parameter Estimation.

Sample No.	$\alpha_s(cm^2 \cdot s^{-1})$	$\varepsilon_s(W \cdot s^{1/2} \cdot cm^{-2} \cdot K^{-1})$
1	0.034 ± 0.002	0.19 ± 0.02
2	0.035 ± 0.001	0.18 ± 0.04
3	0.37 ± 0.02	Not available
4	1.02 ± 0.02	Not available
5	1.4 ± 0.7	0.80 ± 0.03

the thermal effusivity of the samples using Eq. (4), we assumed that the thermal effusivity of the backing, ε_b, is already known [20]. The estimated values show good agreement with the literature values.

Table III shows the results from the amplitude measurements analyzed using three-parameter (f_c, g, and A_0) estimation. The values of thermal diffusivity obtained are reasonable, but the values of thermal effusivity are not reasonable. The "not availlable" in Table III means that the estimated parameter g approaches zero. Because of the strong correlation between f_c and A_0, either of the two parameters should be reduced, as mentioned earlier. In this work, we substituted the f_c values obtained in the phase measurement into the parameter estimation of amplitude measurement. Figure 8 and Table IV show the results. From this, we obtained reasonable values for thermal effusivity.

Table IV. Thermal Effusivity Values Obtained from the Amplitude Measurement by Two-Parameter Estimation

Sample No.	$\varepsilon_s(W \cdot s^{1/2} \cdot cm^{-2} \cdot K^{-1})^a$
1	0.67 ± 0.09
2	0.58 ± 0.04
3	2.2 ± 0.1
4	1.9 ± 0.2
5	2.8 ± 0.3

[a] The f_c value, obtained from the phase measurement, is substituted into this estimation.

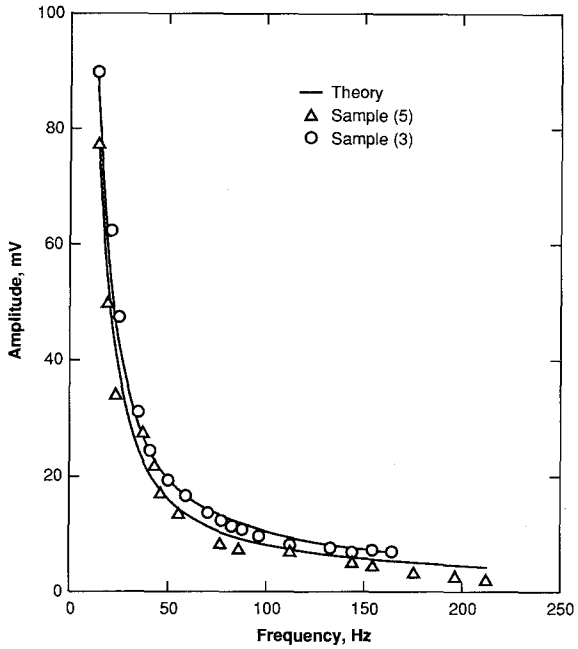

Fig. 8. Experimental data with the theoretical curve fit using the parameter estimation of A_0 and g in amplitude measurement. Sample (3): $A_0 = 45.2$, $g = 0.022$. Sample (5): $A_0 = 34.9$, $g = 0.017$.

6. CONCLUSIONS

The two-layer model developed from R-G theory fits well for the thin metallic sample attached to the plexiglass backing. The parameter estimation technique successfully analyzed the experimental data and provides reasonable values of thermal diffusivity and effusivity. Also, the values of correlation coefficient from the sensitivity analysis show that the theoretical model for phase measurement is more reliable than that for the amplitude measurement. In the parameter estimation of amplitude measurement, the absolute values of the correlation coefficient between f_c and A_0 and between f_c and g are larger than that between A_0 and g. Therefore, when the parameter f_c was removed, PE can give reliable values of thermal effusivity. If we take the ratio of two amplitude values (one for a sample and another for the reference whose thermal properties are already known), the parameter A_0 can be removed. This algorithm will be studied in the next stage.

In order to measure thinner samples, the signal level must be sufficiently strong in the high-frequency region. Therefore, heating by a laser beam is required.

ACKNOWLEDGMENTS

The authors would like to thank Mr. T. R. Goerz for technical assistance, Professor W. M. Becker for experimental help, and ACO Pacific, Inc., for the loan of microphone systems. The first author also thanks the Korea Science and Engineering Foundation for supporting this study.

REFERENCES

1. A. Rosencwaig and A. Gersho, *J. Appl. Phys.* **47**:64 (1976).
2. F. A. McDonald and G. C. Wetsel, Jr., *J. Appl. Phys.* **49**:2313 (1978).
3. N. C. Fernelius, *J. Appl. Phys.* **51**:650 (1980).
4. M. J. Adams and G. F. Kirkbright, *Analyst* **102**:281 (1977).
5. A. Mandelis, Y. C. Teng, and B. S. H. Royce, *J. Appl. Phys.* **50**:7138 (1979).
6. T. Tominaga and K. I. Ito, *Jpn. J. Appl. Phys.* **27**:2392 (1988).
7. A. Lachaine and P. Poulet, *Appl. Phys. Lett.* **45**:953 (1984).
8. G. Benedeta and R. Spagnolo, *Appl. Phys. A* **46**:169 (1988).
9. R. T. Swimm, *Appl. Phys. Lett.* **42**:955 (1983).
10. P. Charpentier, F. Lepoutre, and L. Bertrand, *J. Appl. Phys.* **53**:608 (1982).
11. J. V. Beck and K. J. Arnold, *Parameter Estimation in Engineering and Science* (John Wiley & Sons, New York, 1977), Chaps. 2 and 6.
12. J. J. Hoefler, MSME thesis (Purdue University, West Lafayette, Ind., 1989), Chap. 2, App. C.
13. J. E. Dennis, Jr., M. D. Gay, and R. E. Welsch, *Trans. Math. Software* 7:348 (1981).
14. J. E. Dennis, Jr., M. D. Gay, and R. E. Welsch, *Trans. Math. Software* 7:369 (1981).
15. J. F. McClelland and R. N. Kniseley, *Appl. Opt.* **15**:2967 (1976).
16. N. C. Fernelius, *Appl. Opt.* **18**:1784 (1979).
17. Y. S. Touloukian, *Thermal Diffusivity* (IFI/Plenum, New York, 1973).
18. F. P. Incropera and D. P. DeWitt, *Fundamentals of Heat and Mass Transfer*, 2nd ed. (John Wiley & Sons, New York, 1985), App. A.
19. N. F. Leite, N. Cella, H. Vergas, and L. C. M. Miranda, *J. Appl. Phys.* **61**:3025 (1987).
20. R. S. Quimby, Ph.D. thesis (University of Wisconsin—Madison, Madison, 1979), p. 127.